ARCHIVES OF ACOUSTICS
14, 3–4, 181–190 (1989)

ACOUSTICAL SHADOW OF A SPHERE IMMERSED IN WATER. II

LESZEK FILIPCZYŃSKI, TAMARA KUJAWSKA

Department of Ultrasonics, Institute of Fundamental Technological Research Polish Academy of Sciences
(00–049 Warszawa, ul. Świętokrzyska 21)

Assuming a continuous plane wave incident on a rigid sphere immersed in water the authors computed directivity characteristics of the acoustic pressure behind the sphere. The obtained results were converted and presented in the rectangular coordinate system in the form of acoustic isobars for ka values in the range between 4π and 200π.

Assuming the -6dB isobar to be the shadow boundary, the authors found an almost linear proportionality between the relative shadow range and the ka parameter. The proportionality coefficient was determined and hence a basic formula was given which connects the shadow range, the sphere radius with the wavelength. It can be useful in many ultrasonic problems.

Key words: acoustical shadow, sphere, water, isobar, shadow range.

Przyjmując płaską falę ciągłą padającą na sztywną kulę w wodzie, autorzy wyznaczyli charakterystyki kierunkowości ciśnienia akustycznego za kulą. Uzyskane wyniki przeniesiono w układ współrzędnych prostokątnych w postaci akustycznych izobar dla wartości ka w zakresie od 4π do 200π.

Przyjmując izobarę -6 dB jako granicę cienia, autorzy znaleźli liniowy związek między względnym zasięgiem cienia a parametrem ka. Na tej podstawie uzyskali zasadniczy wzór łączący zasięg cienia, promień kuli z długością fali. Wzór ten może być stosowany w wielu zagadnieniach ultradźwiękowych.

1. Introduction

In the previous papers [3], [2], [1] the authors determined the shadow arising behind a rigid sphere immersed in water for the case of an incident continuous plane wave. Due to axial symmetry computation results were presented in the form of directivity diagrams in two spherical coordinates (r, θ) with angular resolution equal to $\Delta\theta = 1^\circ$ (Fig. 1). The shadow range r_{-6dB}, equal to the distance at which one observs a 6 dB drop relatively to the incident wave pressure, was determined, as well as the corresponding angles to θ_{-6dB} for some ka values.

The purpose of the present paper is the determination of the acoustic pressure field for a greater range of ka values with a higher angle resolution and hence the determination of isobar curves behind the sphere in rectangular space coordinates.

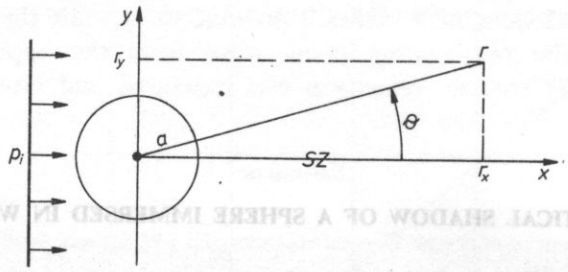

Fig. 1. The spherical coordinate system with the plane wave (p_i) incident on the sphere and the shadow zone (SZ). a – radius of the sphere, r, θ – spherical coordinates, r_x, r_y – projections of r on the symmetry axis x and on the arbitrary axis y, perpendicular to x and passing through the sphere center, respectively

Moreover, the authors intended to generalize the obtained numerical results to present them in the form of a formula enabling simple calculations of shadow range behind the rigid sphere.

2. Acoustic isobars

The acoustic shadow behind the rigid sphere was determined in the previous papers [3], [1] by calculating the acoustic pressure p_s which is equal to the sum of the incident plane wave and the reflected wave pressures. It has the form

$$p_s = \exp(-jkr\cos\theta) - \sum_{m=0}^{\infty} (-j)^{m+1}(2m+1)\sin\eta_m(ka)\exp[j\eta_m(ka)] \times P_m(\cos\theta)h_m^{(2)}(kr), \quad (1)$$

where r, θ are coordinates of the polar system, a radius of the sphere, $k = 2\pi/\lambda$, λ wavelength in the surrounding medium, $\eta_m = \text{arc tan}[-j_m'(ka)/n_m'(ka)]$, j_m', n_m' derivatives of spherical Bessel and Neumann functions, $h_m^{(2)}$ spherical Hankel function, P_m Legendre polynomial, m natural number, $j = \sqrt{-1}$.

In general p_s is a function of the following variables

$$p_s = f(k, a, r, \theta). \quad (2)$$

The dependence on the distance r and on the sphere radius a is represented in Eq (1) by dimensionless products kr and ka respectively. The parameter ka characterizes the shadow form and kr can be considered as a variable. It will be convenient to present the results of our computations in general coordinates introducing the ratio of the two products equal to

$$kr/ka = r/a \quad (3)$$

From Eq. (1) directicity diagrams $p_s = f(\theta)$ were computed for the acoustic pressure behind the sphere for various values of r/a changing the angle by steps equal to $\Delta\theta = 0.1°$. The obtained results were converted and presented in rectangular

coordinates r_x/a, r_y/a in the form of acoustic isobars. They are presented in the lower part of Figs. 2–9 with respect to the acoustic pressure level (0 dB) of the plane continuous wave incident on the rigid sphere. Its center is placed at the origin of coordinates $r_x/a = r_y/a = 0$. The plane wave travels from left to right. On the top of the Figures there are presented angles θ corresponding to the pressure drops of 3, 6 and 9 dB which were obtained from computed directivity characteristics. The r_y/a axis is many times enlarged when comparing with the r_x/a axis. The -6 dB isobars were chosen to be the boundary of the shadow according to our previous definition [3], [1].

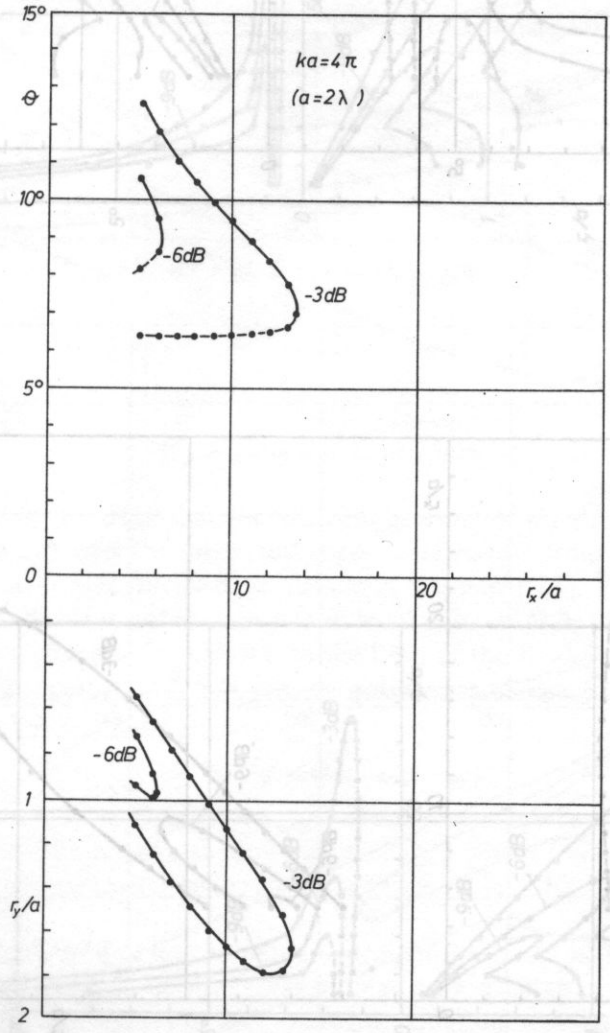

Fig. 2. Angles θ corresponding to adequate pressure drops (top) and acoustic isobars behind a rigid sphere computed for $ka = 4\pi$ (bottom)

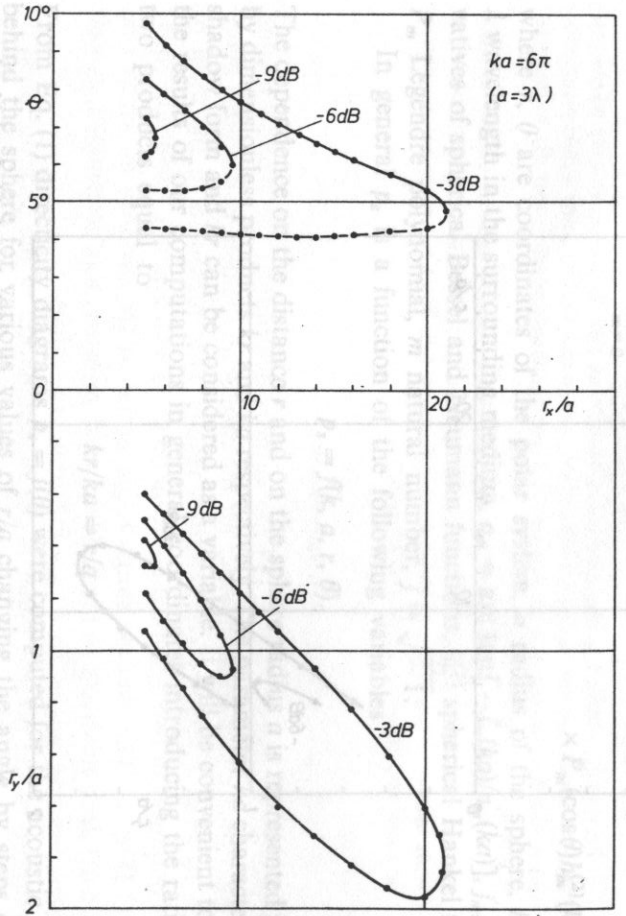

Fig. 3. As in FIG. 2, $ka = 6\pi$

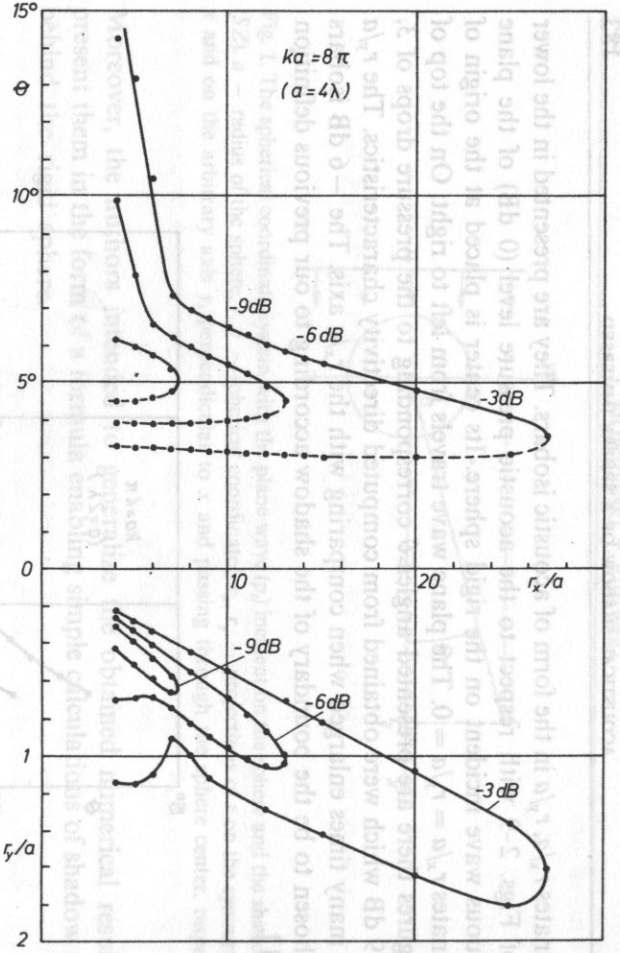

Fig. 4. As in FIG. 2, $ka = 8\pi$

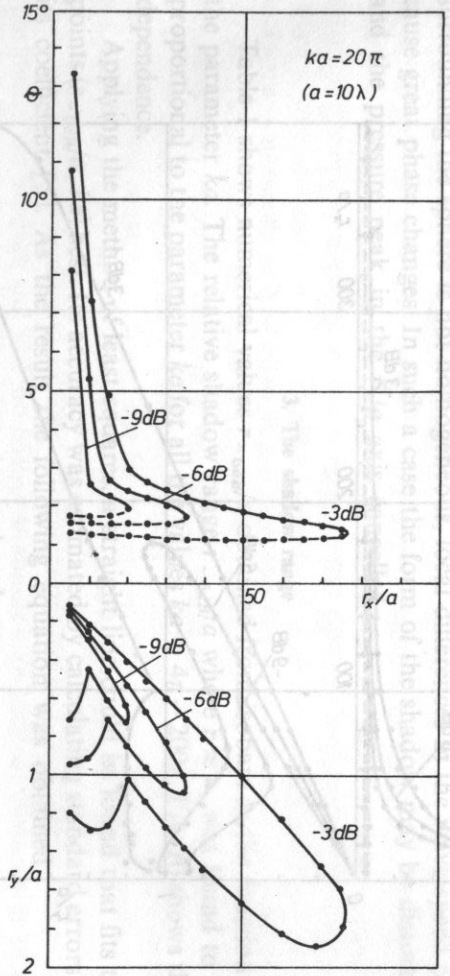

Fig. 5. As in FIG. 2, $ka = 20\pi$

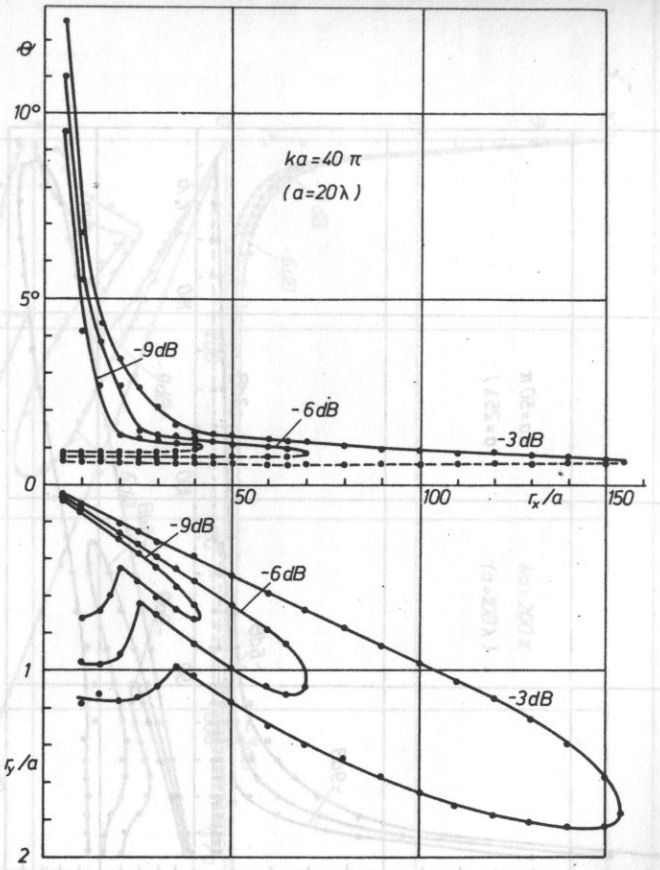

Fig. 6. As in FIG. 2, $ka = 40\pi$

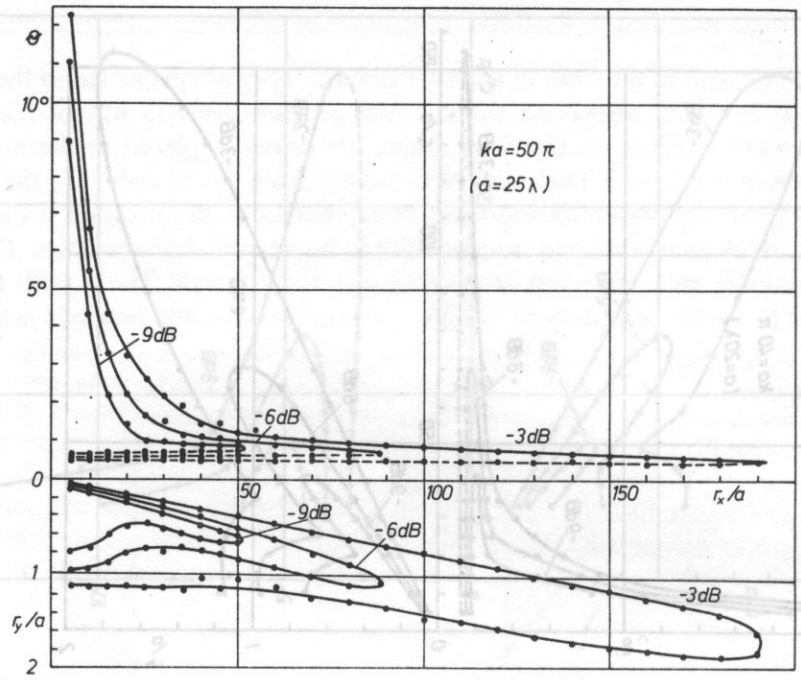

Fig. 7. As in FIG. 2, $ka = 50\pi$

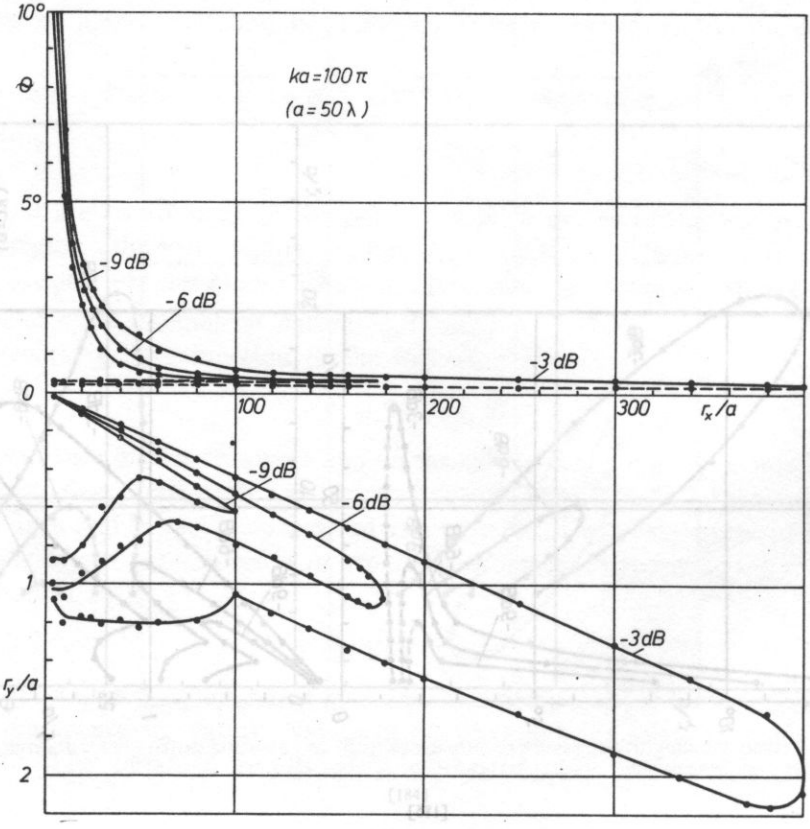

Fig. 8. As in FIG. 2, $ka = 100\pi$

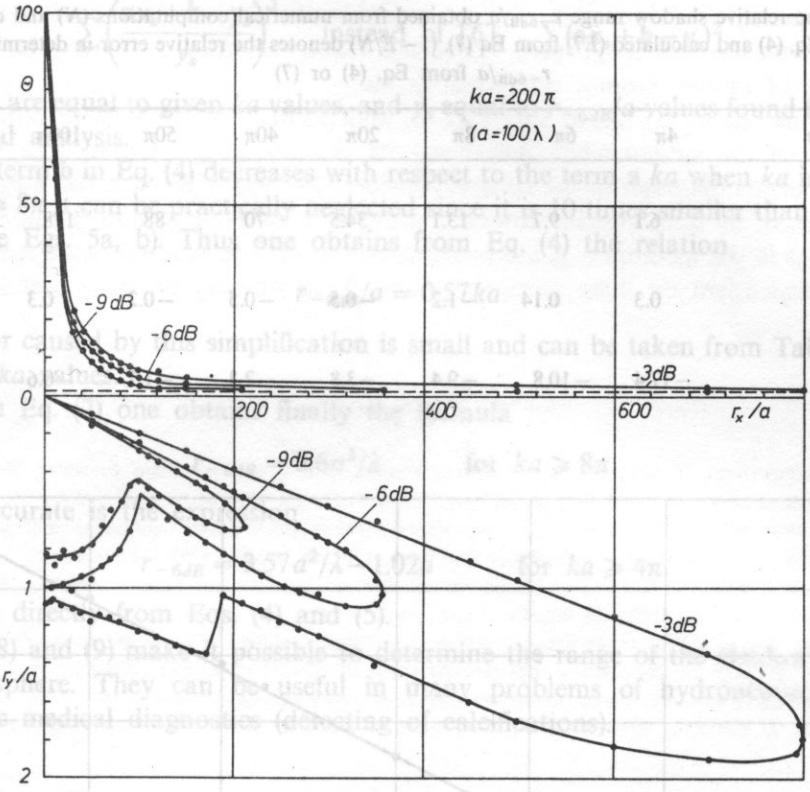

Fig. 9. As in FIG. 2, $ka = 200\pi$

It is interesting to notice that the acoustic pressure along the r_x/a axis is quite large. One does not observe there any shadow. It results from the coherency of acoustic waves, as it was discussed in details in the paper [3]. When the medium surrounding the sphere is not homogeneous, local differences in the wave speed can cause great phase changes. In such a case the form of the shadow may be distorted and the pressure peak in the r_x/a axis cancelled.

3. The shadow range

Table 1 shows numerical values r_{-6dB}/a obtained from isobars as the function of the parameter ka. The relative shadow range r_{-6dB}/a where $r \approx r_x$ was found to be proportional to the parameter ka for all the values $ka = 4\pi - 200\pi$. Fig. 10 shows this dependence.

Applying the method of least squares, a straight line could be found that fits the points $(r_{-6dB}/a, ka)$ best. Its accuracy was estimated by calculating standard errors of its coefficient [5]. As the result the following equation was obtained

$$r_{-6dB}/a = \mathbf{a} \cdot ka + \mathbf{b}, \quad (4)$$

Table 1. The relative shadow range r_{-6dB}/a obtained from numerical computations (N) and calculated ($E4$) from Eq. (4) and calculated ($E7$) from Eq (7). $(1-E/N)$ denotes the relative error in determination of r_{-6dB}/a from Eq. (4) or (7)

ka	4π	6π	8π	20π	40π	50π	100π	200π
$N=\frac{r_{-6dB}}{a}$	6.1	9.7	13.1	34.5	70	88	178	358
$\frac{N-E4}{N}\%$	0.3	0.14	−1.2	−0.5	−0.5	−0.2	0.3	0.6
$\frac{N-E7}{N}\%$	−17.4	−10.8	−9.4	−3.8	−2.3	−1.7	−0.6	−0.04

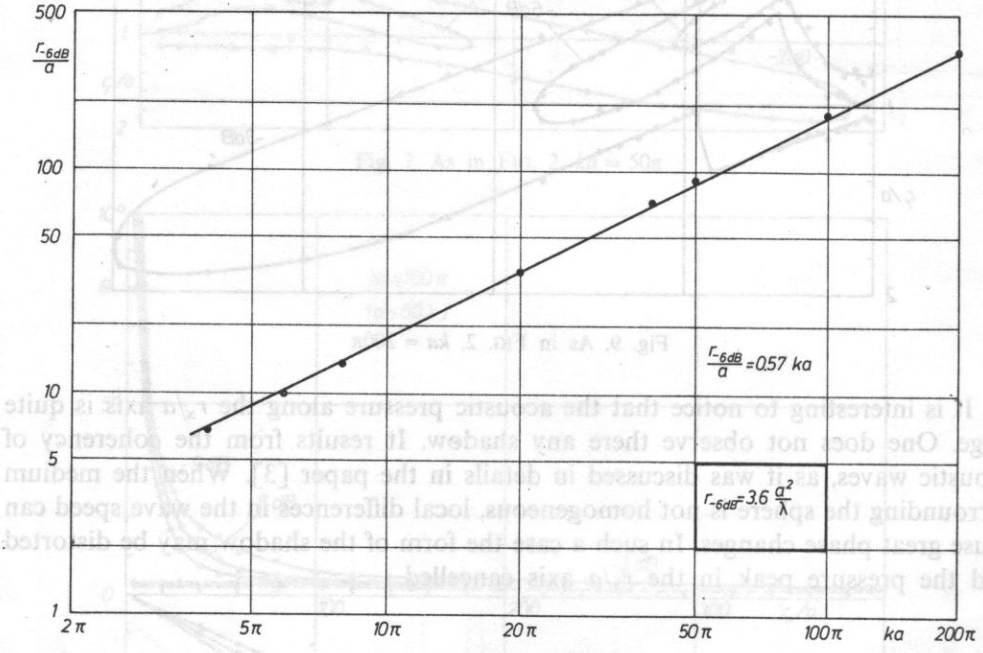

Fig. 10. The dependence of the relative shadow range r_{-6dB}/a on the ka value obtained from numerical analysis

where

$$\mathbf{a} = 0.568 \pm 0.002 \quad \text{and} \quad \mathbf{b} = -1.02 \pm 0.48. \tag{5a, b}$$

This equation was obtained by minimizing the relative error instead of the absolute one, as it is usually realized by a standard procedure. For this purpose we minimized the sum of the squares of the errors

$$\sum\left(\frac{\mathbf{a}x_s+\mathbf{b}-y_s}{y_s}\right)^2 \quad \text{instead of [6]} \quad \sum(\mathbf{a}x_s+\mathbf{b}-y_s)^2, \tag{6a, b}$$

where x_s are equal to given ka values, and y_s equal to r_{-6dB}/a values found from our numerical analysis.

The term **b** in Eq. (4) decreases with respect to the term **a** ka when ka increases. For $ka \geqslant 8\pi$ it can be practically neglected since it is 10 times smaller than the first term (see Eqs. 5a, b). Thus one obtains from Eq. (4) the relation

$$r_{-6dB}/a = 0.57ka. \tag{7}$$

The error caused by this simplification is small and can be taken from Table 1 for various ka values.

From Eq. (7) one obtains finally the formula

$$r_{-6dB} = 3.6a^2/\lambda \qquad \text{for } ka \geqslant 8\pi \tag{8}$$

More accurate is the expression

$$r_{-6dB} = 3.57a^2/\lambda - 1.02a \qquad \text{for } ka \geqslant 4\pi \tag{9}$$

obtained directly from Eqs. (4) and (5).

Eqs (8) and (9) make it possible to determine the range of the shadow behind a rigid sphere. They can be useful in many problems of hydroacoustics and ultrasonic medical diagnostics (detecting of calcifications).

4. Discussion and conclusions

Numerical results of acoustic pressure computation made it possible to present acoustic isobars behind a rigid sphere for a plane continuous wave incident on it and for various ka values in the range between 4π and 200π.

The isobars give an insight into the shadow forming behind the sphere. One should remember that they result as an approximation of calculated directivity diagrams. Fig. 8 of our previous paper [3] gives an example of exact angular distributions of the acoustic pressure behind the sphere. To obtain an adequate isobar it was necessary to draw a mean curve from pressure ondulations arising as the function of the angle θ. However, the applied approximation does not introduce any greater changes in the shape of isobars. The calculation points (Figs. 2–9) were chosen densely enought to obtain the proper shape of isobars.

It was observed that there exists an almost linear proportionality between the relative shadow range r_{-6dB}/a and the ka parameter. The proportionality coefficient could be determined and hence a basic formulae (8) and (9) were found connecting the shadow range, the sphere radius with the wavelength. Their accuracy is quite high as shown in Table 1. The basic formulae (8) and (9) were found to be valid at least for the range of $ka = 8\pi$–200π and $ka = 4\pi$–200π, respectively.

They can be useful in many ultrasonic problems especially in hydroacoustics and in ultrasonic medical diagnostic, where the shadow method is or may be used for detecting of kidney stones, calcifications etc.

It is interesting to notice that Eqs (8) and (9) make it possible to estimate the diameter of the sphere when measuring its shadow range. Up to now the only measure of the diameter of the sphere, considered as the hydroacoustic target, is the amplitude of its echo signal. However, it depends on propagation parameters and conditions in the medium (e.g. attenuation, distance). The shadow range seems to be more independent on these parameters and therefore may be more useful for this purpose.

References

[1] L. FILIPCZYŃSKI, T. KUJAWSKA, *Acoustical shadow of a sphere immersed in water*, Proc. of the V Symposium on Hydroacoustics, Gdynia 1988, 71–78 (in Polish).

[2] L. FILIPCZYŃSKI, T. KUJAWSKA, *Isobar distributions and the shadow range of spheres immersed in water*, Proc. of the VI Symposium on Hydroacoustics, Gdynia, AMW 1989, 115–120.

[3] L. FILIPCZYŃSKI, T. KUJAWSKA, *Acoustical shadow of a sphere immersed in water*. I, Archives of Acoustics, **14**, 1–2 (1989) 29–43.

[4] L. FILIPCZYŃSKI, G. ŁYPACEWICZ, *Estimation of calcification detectability in breast tissues by means of the ultrasonic echo and shadow methods*, Archives of Acoustics, **9**, 1–2 (1984).

[5] H. HÄNSEL, *Podstawy rachunku błędów*, WNT Warszawa 1968 p. 93.

[6] J. TOPPING, *Errors of observation and their treatment*, The Institute of Physics London 1956, p. 101, 105.

Received December 12, 1988.